International Journal of Engineering Research & Technology (IJERT)
ISSN: 2278-0181
Vol. 3 Issue 12, December-2014

Smart Topographies Created by Soft Lithography: Anti-Fouling and Self-Cleaning Engineered Surfaces

Anita Trajkovska Broach
High Performance Optics, Inc., Virginia Tech Corporate Research Center
1750 Kraft Drive, Suite 1300
Blacksburg, VA 24060

Anka Trajkovska Petkoska
University St. Kliment Ohridski-Bitola
Faculty of Technology and Technical Sciences
Dimitar Vlahov bb, Veles,
R. Macedonia

Abstract **- Soft lithography encompasses a collection of inexpensive low-expertise methods to fabricate complex micro- and nano-structured topographies. The most forms of soft lithography use a patterned elastomeric stamp bearing inverse relief features, which can transfer the desired patterns on almost any, flat or curved, surface. The short "turn-around" time from an idea to prototype, coupled with its suitability for a broad range of soft materials and a good control over surface chemistries, has made soft lithography one of the top most versatile fabrication tool in many research laboratories.**

In this work, soft lithographic *replica molding* method was used to fabricate anti-fouling and self-cleaning engineered topographies. Anti-fouling patterned surfaces developed have shown increased inhibition toward bacterial attachment and biofilm formation compared to control surfaces, all made of the same material. The fabrication of self-cleaning hydrophobic topographies, is further proof of the capability and versatility of soft lithography. When these topographies were assessed for their non-wetting and self-cleaning character, most of them have shown the "Lotus-leaf-effect", i.e. water contact angles above 140^{o} and sliding angles between 3-8^{o}. In both types of topographies fabricated in this work, the surface features' size and periodicity seem to play the major role in the surface final performance.

Keywords - Soft lithography, replica molding, antifouling, self cleaning

I. INTRODUCTION

Traditionally, surface patterning in microelectronics has been done with photolithography. However, photolithography has some limitations, such as: it cannot be easily applied to non-planar (curved) surfaces and tolerates a very narrow range of materials with no control over the chemistry of patterned surfaces. The size of features produced by photolithography are dictated by the optical diffraction, while the high-energy radiation needed for small features requires complex facilities and technologies. Photolithography is an expensive technique, often not accessible to non-specialists.

From the other hand, ***soft lithography*** overcomes the limitations of conventional photolithography and further extends its possibilities. Soft lithography is inexpensive and applicable to three-dimensional and curved structures, well-suited for a wide range of elastomeric (soft) materials, such as polymers, gels and other organic materials, which cannot be used in the conventional photolithography. Moreover, soft lithography enables patterning large areas and has a potential for large specific surface area molds and easy fabrication of complex surface patterns and even 3D-networks without expensive capital equipment. It also has a capacity for rapid prototyping, generates well-defined and controllable surface chemistries, and in general, is compatible with biological applications. Thus, soft lithography opens novel applications in biotechnology, flexible electronics, microfluidics, etc. [1-14]

Soft lithography is a process in which a soft polymer (elastomer) is cast onto mold that has the desired surface pattern. The elastomeric "soft" mold or stamp in soft lithography is made from a master or template, which is most often fabricated on a silicon wafer by conventional lithography. *Figure 1* below is a schematic presentation of a master, which is used to make an elastomeric stamp by solidifying the liquid prepolymer material with heat or UV light.

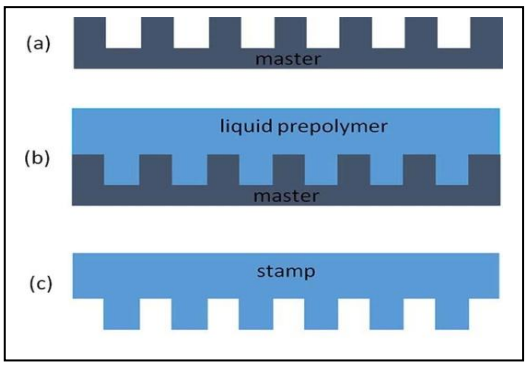

Figure 1. Elastomeric stamp fabrication from a rigid master.

The elastomeric stamp is a key in soft lithography, because it is used to generate the desired surface patterns. The stamp is made usually of a soft material, very often polydimethylsiloxane (PDMS). PDMS has been the most widely used material as stamp material in soft lithography due to its outstanding properties, such as low cost, transparency, biocompatibility, low toxicity, chemical inertness, diverse surface chemistry, mechanical flexibility and durability, as well as low viscosity before curing, which is usually by thermal means. Various acrylates, mostly photo- curable, have been also used as stamp materials in soft lithography. The soft

and rubbery backbone of PDMS and other elastomers enables conformal contact that is crucial for a good reproduction of desired patterns in soft lithography.

According to Whitesides *et al.*, the terminology *soft lithography* does not refer to a unique fabrication technique, but it is *"a collection of techniques based on printing, molding, and embossing with an* ***elastomeric stamp*** [1-6]. Some of the soft lithographic fabrication methods, which use a patterned elastomeric stamp are given below:[15-20]

- Replica molding,
- Micro-contact printing,
- Micro-transfer molding,
- Micro-molding in capillaries,
- Solvent-assisted micro-molding,
- Micro-particle fabrication,
- and many variations of the above methods.

Schematically, several soft lithographic techniques are given in *Figure 2*.

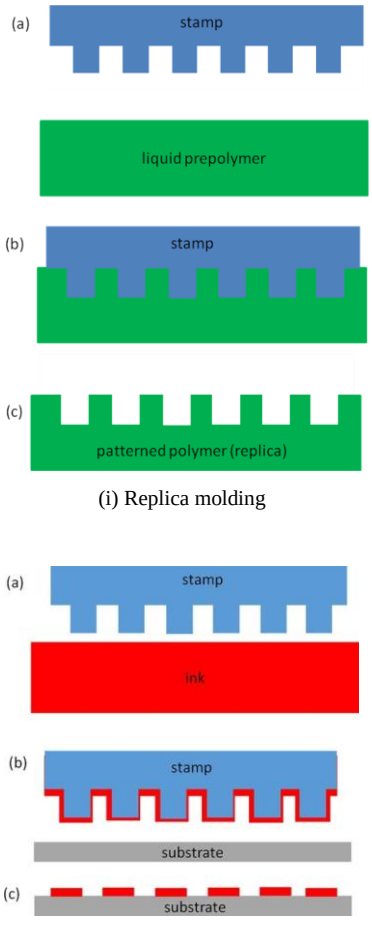

(i) Replica molding

(ii) Micro-contact printing

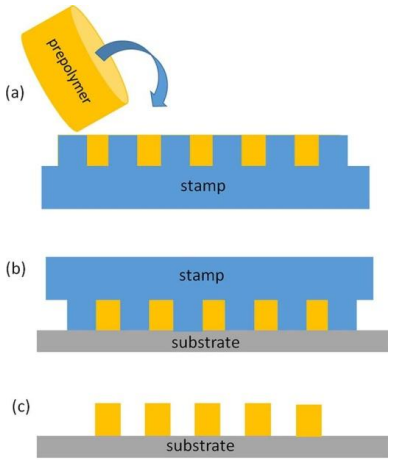

(iii) Micro-transfer molding

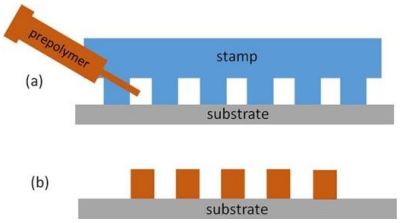

(iv) Micro-molding in capillaries

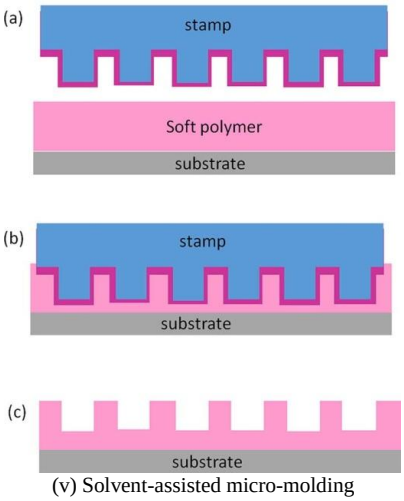

(v) Solvent-assisted micro-molding

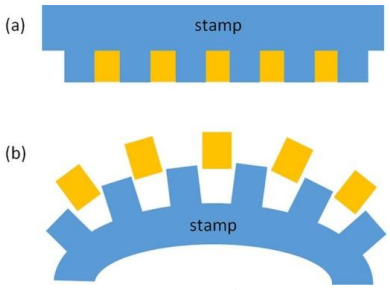

(vi) Micro-particle fabrication

Figure 2. Soft lithographic techniques: (i) replica molding; (ii) micro-contact printing; (iii) micro-transfer molding; (iv) micro-molding in capillaries; (v) solvent-assisted molding; and (vi) micro-particle fabrication.

In ***replica molding*** (*Figure 2i*)**,** a patterned elastomeric stamp is used as a soft mold and filled with a liquid prepolymer. Upon curing the prepolymer by heat or UV light, the cured polymer is easily separated from the stamp due to low surface energy of the stamp. The inverse patterns of the stamp are imprinted in the surface of the polymer, known also as replica. Replica molding allows replicas to be made in a wide spectrum of materials and the stamps to be reused many times.

In ***micro-contact printing*** (*Figure 2ii*), the stamp is first soaked in a molecular "ink", and then brought into contact with a substrate, where the ink patterns transfer onto the substrate surface. It should be noted that in micro-contact printing, only the ink from the raised surface patterns of the stamp is transferred to the substrate, which has higher surface energy than the stamp material.

In ***micro-transfer molding*** (*Figure 2iii*), the stamp patterns are filled with liquid prepolymer. Upon partial or full curing of the prepolymer, the filled stamp is brought in contact with a substrate that has higher surface energy than the stamp, and thus, the partially- or fully- cured polymer patterns are transferred onto substrate surface. In the case of partially-cured polymer, the patterns can be additionally cured on the substrate.

Capillary molding or micro-molding in capillaries (*Figure 2iv*) is another technique, where a patterned elastomeric stamp is used as a mold. First, the patterned surface of the stamp is brought into contact with a substrate. Then, the patterns of the stamp are filled with a liquid prepolymer. Capillarity is used to progressively fill the patterns, but suction can be used, as well. After curing of the polymer, the stamp is easily removed due to its low surface energy, leaving solid micro-structures on the surface of the substrate.

Solvent-assisted micro-molding (*Figure 2v*): The stamp is initially wet with a solvent that swells the polymer intended to be patterned. Upon the stamp is brought into contact with the polymer, a thin layer of the polymer is dissolved (swollen) and conforms to the mold pattern. After solvent evaporation, the polymer solidifies into desired patterns and the low surface energy stamp is removed.

Beside patterned topographies, ***tailored micro- and nano-particles*** (*Figure 2vi*) can be fabricated with soft lithography. The cavities of the elastomeric low surface energy patterned stamp are filled with liquid prepolymer. Upon curing (thermal- or photo-curing), the formed micro-particles from the stamp cavities can be released and collected [21].

In this study, among many patterned topographies fabricated, only two categories of engineered surfaces will be disclosed. The first category of patterned engineering surfaces disclosed in this study are anti-fouling topographies, i.e. surfaces with such topographic features that reduce bacterial colonization and biofilm formation. The second category of disclosed engineered topographies are related to self-cleaning hydrophobic surfaces.

II. EXPERIMENTAL

Micro-patterned topographies were prepared by soft lithographic method ***replica molding*** (*Figure 2i*) using micro-patterned acrylic-based stamps. The stamps were originally prepared from the master fabricated by the conventional photolithography and were reused many times (> 50 times). The photo-curable acrylate/methacrylate formulations used for making the stamps were designed in such way to provide certain degree of flexibility for a good conformal contact and release from the replicas, but also some rigidity for easy handling, especially when large area stamps were needed. The micro-patterned replicas were made in different photo-curable liquid prepolymers based on acrylate-urethane- and fluoro-acrylate polymer formulations. Depending on the intended final application, different prepolymer formulations were used. A fluoro-acrylate and an acrylate-urethane formulation were used for the fabrication of anti-fouling topographies, while several fluoro-acrylate formulations were used for making non-wetting hydrophobic surfaces. The actual chemical compositions of the stamp polymer formulations used in this study, as well as the actual chemistry of the replica polymeric materials will be not disclosed here due to proprietary reasons.

Some of the patterned surfaces made by soft lithography were further subjected to reactive ion etching (reactive ion etcher, Trion Technology Phantom II) in order to impose dual structure topographies, i.e. random nano-structures embedded on top of the micro-structures. For comparative purposes, reactive ion etching was applied on smooth surfaces made from the tested materials resulting in random nano-structured topographies only.

Topographic characterization of micro-patterned stamps and patterned surfaces (replicas) was done with scanning electron microscopy, SEM (FEI XL30 SEM-FEG).

The anti-fouling engineered surfaces were further characterized in terms of monitoring the bacterial growth on them over certain time period (1-60 days) and conditions (temperature, humidity, flow and static conditions) and were compared to smooth surfaces made of the same materials as control surfaces. The surface energy of smooth surfaces was determined by commercially-available ***ACCU DYNE TEST™*** marker pens. The anti-fouling character of the surfaces developed in this study was tested against two strains of bacteria, *Escherichia coli* as gram-negative bacteria and *Staphylococcus aureus* as gram-positive bacteria, in static and flow conditions. The static conditions were improvised in large plastic containers (*length x width x depth* = 0.5 x 0.5 x 0.5 m), coated and patterned with the studied materials and topographies, and filled with stagnant water. The dynamic conditions were improvised on plastic plates containers (*length x width* = 0.5 x 0.5 m), coated and patterned with the studied materials and topographic features, over which water was allowed to pass with velocities of 0.1 - 1 m/min.

The self-cleaning hydrophobic surfaces were characterized for their self-cleaning and repelling performance of water drops. The wettability of the replicas was characterized by contact angle measurements (Drop Shape Analyzer – DSA100S, KRUSS). Water droplets (5 µl) were applied to the studied surfaces with a syringe. The sliding angles were measured by tilting the engineered surfaces with applied droplets on them. Particularly, the minimum angle at which the droplets rolled-off the surface without wetting it (i.e. without spreading on the surface) was recorded as a sliding angle for the particular surface. For this purpose, the tested surfaces (*length x width* =

0.5 x 0.5 m) were covered with sand comprising micron-sized particles in amount of 0.02 g sand/cm^2 surface and were microscopically inspected before and after water drops roll over them for qualitative observation of the washed/non-washed sand particles. The water droplets were supplied at the top edge of the tested surface in amount of 10 ml/cm^2 surface.

III. RESULTS AND DISCUSSION

A. *Anti-fouling micro-structure based topographies*

Bacterial surface fouling (bacterial attachment) and biofilm formation are big problems in many applications and industries, including but not limited to: medical devices (implants, replacement joints, stents, pacemakers, catheters), municipal infrastructure (drinking water pipes, wastewater treatment), food production (food processing surfaces, processing equipment), hospitals, water transportation vehicles (ships), etc. [22-42] Biofilms are considered to be a collection of microorganisms surrounded by the slime they secrete, attached to a surface. Biofilm is defined as "*structured, co-operative microbial community embedded in an extracellular usually polysaccharide matrix, attached to a surface.*" Biofilms that we all are familiar with are the plaque on the teeth, the slippery slime on river stones, the gel-like film inside the vase which hold flowers for a week, etc. Biofilm exists wherever surfaces are in contact with water or body fluids. The stages in biofilm formation on surfaces are schematically given in *Figure 3*.

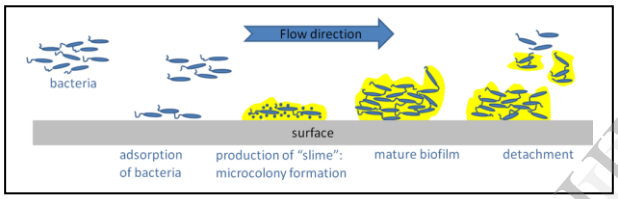

Figure 3. Stages of biofilm formation on surfaces.

The most dangerous biofilms by far are those formed on medical devices, tubes and surfaces. [32-35,38-41] For instance, catheter-related infections are often associated with the bacterial growth and biofilm formation in catheter tubing. Broad-spectrum antibiotics are often initially implemented to reduce the risk of hospital-related infections and patient mortality, which means increased cost, complications for the patient, but also undesirable increased risk for antibiotic resistance. For instance, pneumonia is the most common hospital-acquired infections in intensive care units responsible for almost 1/3 of all infections and requires more than 50% of all the antibiotic prescriptions in the intensive care units.

Furthermore, the presence of microbial cells on a metal surface can cause the so-called microbiologically influenced corrosion or bio-corrosion [36,37]. Bio-corrosion is a result of non-uniform colonies of bacteria, which result in formation of differential aeration cells i.e. the areas under the colonies are depleted of oxygen relative to the surrounding non-colonized areas. Different oxygen concentrations at two locations on a metal cause a difference in electrical potential, and consequently, existence of corrosion currents. Even stainless steel relies on a stable oxide film to provide corrosion resistance. When this oxide film is damaged or oxygen is kept from the steel surface, corrosion happens even in the stainless steel. Moreover, some types of biofilm bacteria produce corrosive chemicals, like acids and hydrogen gas, during their metabolism, which can be detrimental for metal surfaces.

To avoid the danger of biofilm formation, several solutions have been proposed to prevent bacterial attachment and biofilm formation on various surfaces [42-51]. One way is to add antibacterial chemicals (e.g. antibiotics or other anti-microbial agents), which are not always applicable due to their toxicity and side effects for humans, ocean flora and fauna, the risk of development of antibiotic resistance, etc. Another anti-fouling strategy utilizes engineered topographical features on surfaces in contact with water/body fluids to reduce bacterial bio-fouling, and therefore, limit the ability of individual cells to attach to the surface, colonize, and form biofilms.

The later anti-fouling strategy of engineered topographies is a part of this report in "fighting" biofilm formation on plastic surfaces or this purpose. For this purpose, surface patterns that were anticipated to disrupt the ability of bacteria to adhere, colonize, and develop into biofilms were fabricated by soft lithographic technique *replica molding*. An example of a fabricated topography by replica molding is given in *Figure 4*. Particularly, SEM image of an engineered surface with square posts is given in *Figure 4a*, while the SEM of the elastomeric stamp used to make such surface is presented in *Figure 4b*.This approach of suppressing biofilm formation based solely on micro-patterned topographies seems to be the best in fighting bacterial growth and contamination on surfaces of interest without any toxic anti-microbial chemicals and antibiotics, and thus, without any harmful consequences for the life.

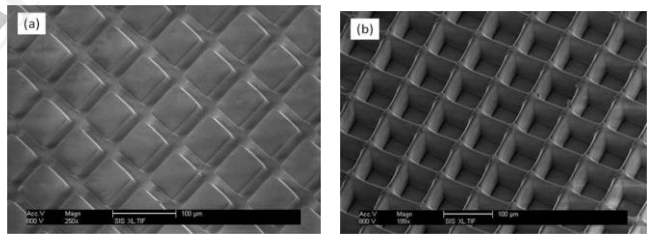

Figure 4. SEM images of (a) micro-patterned replica produced by soft lithography and (b) elastomeric stamp used to make the replica (a).

The engineered patterned surfaces were made of both materials used in this study, acrylate-urethane and fluoro-acrylate polymers. Besides the well-defined patterned surfaces, the biofilm formation rate was monitored on randomly patterned surfaces (*Figure 5*) fabricated also by replica molding technique. The random features were made to have sizes on very different scales, as can be seen by comparison of *Figures 5a* and *5b*.

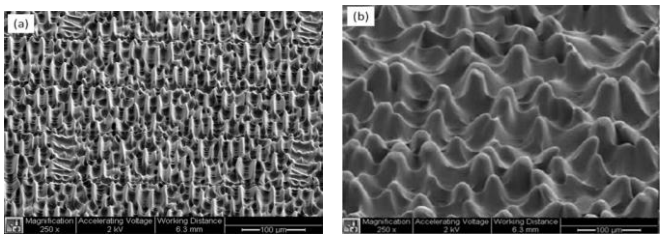

Figure 5. SEM images of a random-structure topographies used in this study and produced by soft lithography.

It is known that the bacterial adhesion to surfaces is greatly affected by the physical and chemical properties of the surface, as well as the characteristics of the bacteria. The authors believe that the results of the kinetics study of bacterial attachment on tested surfaces are beyond the scope of this paper, which is the versatility of various soft lithographic methods. However, some of the bacterial growth kinetic study results will be briefly mentioned here with the purpose to present the intended applications of the fabricated topographies by soft lithography. The initial results of the kinetic study have shown that the topographical features developed in this study reduced cell-surface interactions, and thus, reduced surface colonization and biofilm formation compared to smooth surfaces made of the same materials. Furthermore, the results showed that the kinetics of bacterial attachment to the tested surfaces was slightly affected by the surface energy of these materials, when smooth surfaces were tested. Particularly, two types of materials were tested: smooth surfaces made of acrylate-urethane material and fluoro-acrylate materials with surface tension values of 45 mN/m and 25 mN/m, respectively. In both cases the biofilm was formed; however, fluoro-acrylate surfaces had less amount of biofilm formation than the acrylate-urethane-based smooth surfaces for a given time period. Therefore, surface material nature has little or no effect on biofilm formation rate; the lower surface energy material inhibits the initial bacterial attachment compared to the higher surface energy material.

The random structured surfaces showed significant reduction in bacterial attachment to the surface compared to the smooth surfaces, but not as good as the well-defined patterned surfaces. The ordered patterned surfaces showed the most reduced bacterial attachment compared to all tested surfaces. Preliminary results on kinetics of biofilm formation showed that the size, spacing, and shape of surface features play a significant role in cell-surface attachment. Therefore, antifouling strategies that utilize engineered *topographical features with well-defined dimensions and shapes* (*Figure 4*) demonstrated the highest degree of controllable inhibition over bacterial attachment, when compared to smooth surfaces or randomly-texturized surfaces (*Figure 5*).

Among different well-defined topographic features tested in this study, the best results were observed for square- and cylindrical- micron-sized posts. In *Figure 4a*, the SEM image of square-like posts only is given.

To assess the effect of the surface patterns' size and shape on kinetics of bacterial attachment, various topographic features were fabricated and tested. For this purpose, the pitch *p* (or period), width *w* and height *h* of square- and cylindrical posts were systematically changed and easily prototyped by soft lithography (*Figure 6*).

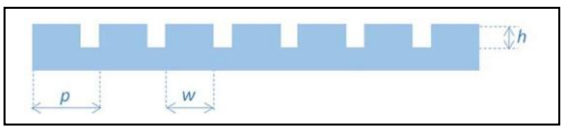

Figure 6. Schematic of a cross-section of topographies developed and studied as anti-fouling surfaces.

For patterned topographies with square posts, the pitch *p*, was changed as a function of the feature width *w* (equation 1), in the range given below:

$$w + w/4 \leq p \leq 2\,w \qquad (1)$$

while the height *h* was varied in the range given with the equation 2:

$$w/4 \leq h \leq w/2 \qquad (2)$$

For cylindrical posts, the same equations given above were used with *w* equal to the post diameter.

The cell attachment was observed to be strongly dependent upon the size and periodicity of topographical features under both, static and flow conditions. With other words, since the periodicity and the size of the features affects the specific surface area, the mathematical correlation between the specific surface area and initial biofilm formation is envisioned.

The surface patterns were tested against two different strains of bacteria, *Escherichia coli* as gram-negative and *Staphylococcus aureus* as gram-positive bacteria. No statistical difference in the rate of surface attachment between gram-positive and gram-negative bacteria on tested topographies was observed.

In regard to the flow conditions, biofilm was formed in both, static and dynamic conditions. The initial observation was that even a high flow rate did not prevent bacterial attachment nor completely remove the existing biofilm, but it limited the total biofilm thickness only. The reason for this is believed to be that even in turbulent flow conditions, there is always a laminar sublayer close to the surface, which allows the bacteria to attach to the surface and progress into biofilm. In turbulent conditions, it is expected that the biofilm fragmentation and detachment would happen more often, resulting in lower total biofilm thickness compared to laminar flow conditions.

As stated above, the extensive results of the kinetic studies of biofilm formation will be not reported here and will be published additionally. Without reporting the results on the quantitative assessment of biofilm formation on tested topographies, the key qualitative observations from the initial biofilm studies are as follows:

- *Material surface energy*: surface material nature has little or no effect on biofilm formation rate;
- *Specific surface area*: well-defined engineered topographical have demonstrated the highest degree of controllable inhibition over bacterial surface attachment when compared to smooth surfaces or randomly-texturized surfaces. The specific surface area of surface patterns (i.e. their period and size) plays the major role in the kinetics of biofilm formation;
- *Bacteria type*: no statistical difference in the bacterial growth rate on tested surfaces was observed for *Escherichia coli* and *Staphylococcus aureus;*
- *Flow conditions*: biofilms were formed in both, static and dynamic conditions, with only difference in the final biofilm thickness, which appeared to be thicker in static and laminar conditions.

B. Self-cleaning hydrophobic engineered surfaces

Inspired by the self-cleaning and superhydrophobic examples in Nature, several topographies that resemble plants' leaves and petals were developed in this study by soft lithography. Self-cleaning and superhydrophobic surfaces that repel various liquids without wetting the surface can find use in a wide range of technological and consumer applications, including self-cleaning windows, windshields, sun rooms, glass roofs, repellent fabrics, anti-icing surfaces, drag-reducing surfaces, solar panels, utensils, etc.

To-date, many plants and animals from the nature have been extensively investigated for their non-wetting and superhydrophobic character. Most of the studied non-wetting plant leaves, butterfly and insects' wings, animals' skins and shells have been found to have well-structured topographies in addition to the low-surface-energy material that they are composed of [52-86].

One of the most studied examples in Nature is the ***lotus leaf*** (*Nelumbo Nucifera*), known for its superhydrophobicity and self-cleaning effect (*Figure 7*). Also known as sacred lotus, lotus leaf has been known as a symbol of purity in Asian culture for over 2,000 years due to its capability to remain clean. Due to its extreme water repellency and self-cleaning performance, lotus leaves always remain clean in muddy and dirty ponds; such effect is often known as the '*Lotus Effect*' in literature [70-76]. Particularly, the water drops are rolling over the top of leaf hierarchical structures made of low surface energy epicuticular wax and maintaining their droplet shapes. The reason for this is that there isn't enough surface contact area for the adhesive forces of the surface to overcome the cohesion forces in the water droplets and spread them on the surface. Therefore, the dust and debris on top of the surface features are most likely to be attracted more by the polar water molecule than to the low energy wax surface (*Figure 7b*). The phrase *Lotus-Effect*® has been even registered as a trade-name for self-cleaning superhydrophobic micro- and nano-structured surfaces.

Figure 7. (a) Superhydrophobic lotus leaf (*Nelumbo Nucifera*) with drops rolling on but not wetting the surface. (b) Graphic presentation of the self-cleaning property of lotus leaf surface (Wikipedia).

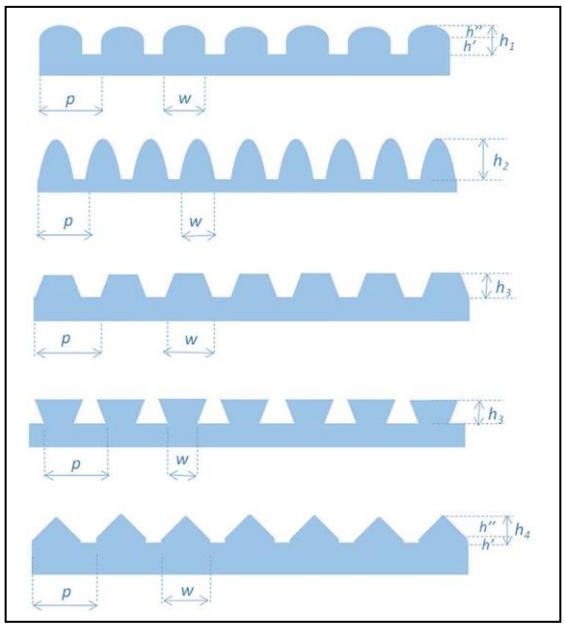

Figure 8. Schematic of cross-sections of different topographies developed and tested for their self-cleaning hydrophobic performance.

The self-cleaning action of superhydrophobic surfaces originates from their high water contact angles; water on these surfaces usually forms spherical droplets, which roll away collecting and carrying the dirt from the surfaces. The rolling motion of the droplets is crucial in the self-cleaning process. The droplets and their *rolling motion* are cleaning the surface more efficiently and is less likely to leave behind dirt than the *sliding motion*, when droplets spread-out, which usually occurs on surfaces with lower contact angles. Besides some inconsistencies, many authors have agreed that the general requirements for a self-cleaning hydrophobic surface are:

- ***a high water contact angle*** (often stated to be above 150^{o}), and
- ***a very low sliding angle*** (also, known as roll-off angle), i.e. minimum inclination angle necessary for a droplet to roll-off the surface (often stated to be less than 5^{o}).

Repellent superhydrophobic surfaces can be actually designed either by selecting low surface energy materials, or by introducing surface patterns, or both [88-98]. With a specific objective to fabricate non-wetting engineered topographies in an easy and inexpensive way, soft lithography was utilized to produce micro-structure-based patterned surfaces. The cross-sections of soft-lithographic patterned surfaces developed in this work are given in *Figure 8.* These surfaces were developed to provide different specific surface areas, and thus, different contact areas between the liquid drop and the surface. The effect of the shape and size of surface features on so-called "air-trapping phenomenon"[74] was considered, as well.

The sizes of surface features in this work were systematically varied. Particularly, the pitch or period *p*, and the height *h*, of micro-structures were varied as functions of the width *w*, as given with equations 3-13 below:

$$w \le p \le 2w \quad (3)$$

$$0 \le h' \le w/2 \quad (4)$$

$$w/4 \le h'' \le w/2 \quad (5)$$

$$h' + h'' = h_1 \quad (6)$$

$$w/4 \le h_1 \le w \quad (7)$$

$$w/2 \le h_2 \le 2w \quad (8)$$

$$w/2 \le h_3 \le w \quad (9)$$

$$0 \le h' \le w/2 \quad (10)$$

$$w/4 \le h'' \le w/2 \quad (11)$$

$$h' + h'' = h_4 \quad (12)$$

$$w/4 \le h_4 \le w \quad (13)$$

In addition to the topographies given in *Figure 8* above, random topographies, which SEM images are given in *Figure 5*, were tested for their hydrophobic and self-cleaning performance.

The engineered repellent hydrophobic topographies were fabricated in laboratory settings by soft lithographic *replica molding* technique. The precise chemical composition of the materials used for these engineered surfaces will be not disclosed here due to the proprietary reasons. In general, the materials used for fabrication of self-cleaning superhydrophobic topographies were different photo-curable fluoro-acrylate formulations due to their intrinsic lower surface energy. The surface energy measured on flat surfaces of these materials (i.e. surfaces without any structures) was in the range 20-25 mN/m. Besides the chemical composition, a minor effect on the surface energy of surfaces was observed by the curing process, i.e. the total UV fluence used for curing the fluoro-acrylate formulations. The contact angle measurements yielded that all tested surfaces have shown water contact angles of 140^o or greater.

In some cases, the soft lithographic fabrication of micro-structured surfaces was followed by reactive ion etching post-fabrication step with CFx/O_2 gasses for different time periods in order to create dual-structure topographies (random nano-structures imposed on top of micro-structured surfaces).

In *Figure 9* are given SEM images of surfaces of petals and leaves of *Dahlia*, *Rosa montana*, and *Colocasia esculenta* plants (*Figure 9a*, *9c* and *9e*) and artificial engineered topographies made by soft lithography followed by reactive ion etching (*Figures 9b*, *9d* and *9e*). The close resemblance of the artificial surface structures made in our laboratory, to the surface structures found in Nature (e.g. compare *Figures 9a* and *9b*) confirms the primary goal of the study: a relatively inexpensive soft lithographic step followed by reactive ion-etching step yielded the intended dual structure topography. By adjusting the conditions of both steps in the fabrication process (the surface chemical formulation and its photo-curing, the etching gas type and the etching time), one can produce tailored surfaces in terms of their patterns and performances.

Plant surfaces from Nature ***Surfaces made by soft lithography***

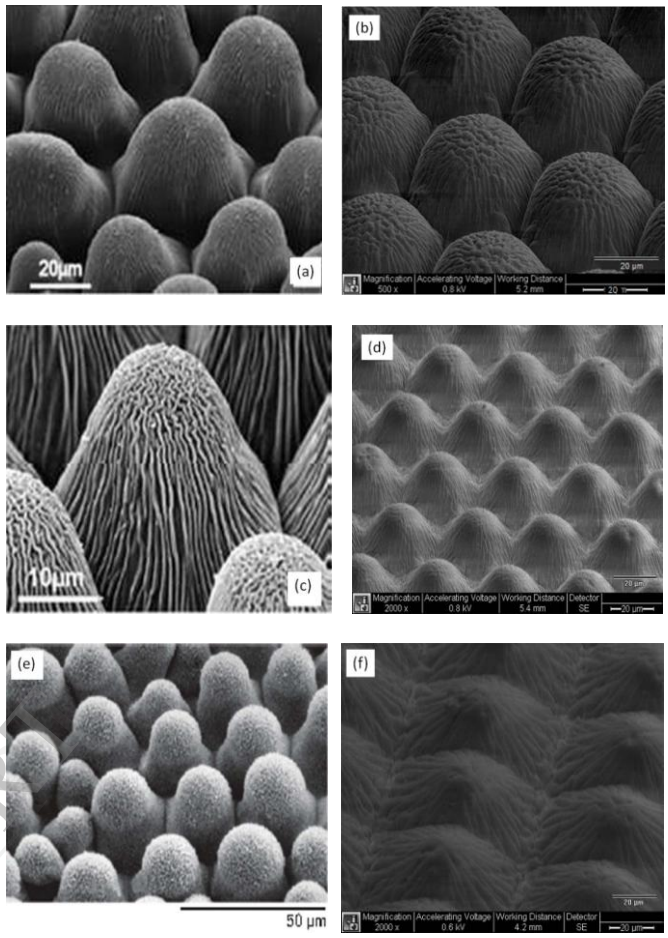

Figure 9. SEM images of plant surfaces found in nature (left column) and surfaces produced in this study by soft lithography (right column). (a) *Dahlia petal*, (c) *Rosa montana*, and (e) *Colocasia esculenta* (elephant's ear), adapted from Ref. [86, 87]; (b), (d) and (f) artificial surfaces developed in this study by soft lithography followed by reactive ion etching.

So far, several groups have been able to produce replicas of lotus leaf and other plants' leaves by direct replication on those leaves, or by other methods creating superhydrophobic patterns similar to those found in Nature. [69,88-98] To the best of our knowledge, the present study is the first report of engineered dual structure surfaces, very close to the surfaces found in Nature, and fabricated by soft lithography using "artificial" elastomeric stamps. The various surface micro-patterns, which cross-sections are schematically given in *Figure 8*, were easily prototyped by replica molding. The replicas, which SEM images are given in *Figure 9b*, *9d* and *9e*, are just three examples of topographies made in our laboratory by replica molding followed by reactive ion etching. Many more topographies were fabricated by soft lithography with an objective to study the effect of patterns' pitch and size on surface self-cleaning and hydrophobic character. For instance, all replicated surfaces given in *Figure 9* have pitch *p* equal to the pattern's width *w* (*p* = *w*). Among all studied topographies, where p was chosen to be in the range between *w* and *2w*, the topographies with p equal or

closer to *w*, have shown the best results in terms of self-cleaning performance. The self-cleaning effect was found to be closely related to the relative ratio of the size of the water drop on top of the tested surface with respect to the pattern's pitch and size. In-depth details from the study on the self-cleaning and superhydrophobic effects of tested topographies will be published additionally. The authors believe that these results are beyond the scope of this report.

By changing the etching conditions, one can made variety of nano-structures in combination with micro-structures, as presented in *Figure 10.* The longer period of reactive ion etching yielded more pronounced nano-structures, i.e. nano-structures embedded deeper into the micro-structures. The topography presented in *Figure 10a* is made by etching time of micro-structured surface for 30 s with CF_4 : O_2 = 1 : 1, while the topography given in *Figure 10b* is made by etching time of 120 s with the same gas mixture and under the same other conditions as the surface in *Figure 10a*.

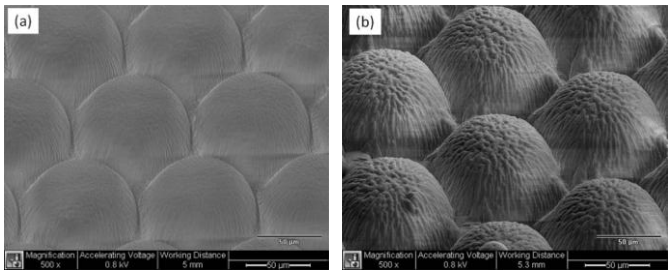

Figure 10. SEM images of topographies made by soft lithography followed by reactive ion etching with CF_4/O_2 for: (a) 30 s and (b) 120 s.

Micro-structured and hierarchical micro-/nano-structured topographies developed in this study were subjected to measurement of their non-wetting character towards water. Besides the qualitative observation of the repellency and assessment of the contact angles on different surfaces, the engineered surfaces were assessed for their self-cleaning character, as well. Upon being covered with sand comprising micron-sized particles (0.02 g sand/cm^2 surface), the tested surfaces were tilted at given angles and subjected to water droplets, supplied at the top edge of the tested surface (10 ml/ cm^2 surface). *Figure 11a* presents a schematic of this assessment: drops of water were supplied on the top edge of each tested surface containing sand particles. The tested surfaces were observed under microscope before and after the water washing step. For superhydrophobic surfaces, the water drops rolled down the surface as spherical drops, which collect the sand particles from the surfaces (*Figure 11b*). On the surfaces with lower hydrophobicity, the water drops were not spherical, i.e. they spread out and their "cleaning performance" was not as good as in the case of superhydrophobic surfaces (*Figure 11c*). The minimum angle α (*Figure 11a),* at which the water still rolls-off from the surface without spreading on the surface was registered for each surface. This angle α was reported as a sliding angle for each of the developed engineered topographies. All tested topographies have shown sliding angles in the range 3^o-8^o.

It is believed that the self-cleaning property is due to the stronger adhesion between the water droplet and the particles than the adhesion between the particles and the surface, hence the spherical water drops pick up the particles while rolling-off. On micro-structured and dual micro-/nano-structured surfaces, water drops are "tip-toeing" over the tops of the surface patterns and maintaining their droplet shapes, because there isn't enough surface area for the adhesive forces of the surface to overcome the cohesion forces in the water. Therefore, the sand particles "sitting" on top of the surface features are most likely to be attracted more by the water (as a polar molecule) than to the low energy surface. This effect is similar to what is happening on lotus leaf surface, which always appears to be "perfectly" clean (*Figure 7*).

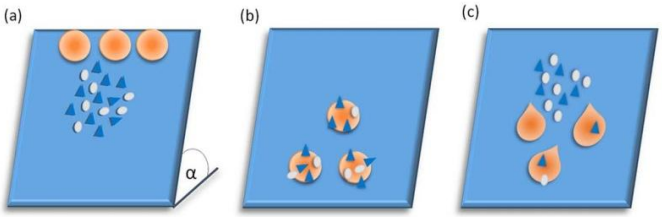

Figure 11. (a) Water drops on tilted surface covered with sand particles; (b) water drops rolling-off on tilted superhydrophobic surfaces and collecting the sand particles; and (c) water drops spreading on lower surface energy surface and leaving behind the particles.

Actually, the experimental results confirmed that the water drop wets or does not wet the flat surface of a given material as dictated by the material surface energy *(Figure 12a*). By introducing surface structures, the wetting character of the surface of the given material can be further modified. In *Figures 12b* and *12c* are given surfaces with nano-structures only and micro-structures only, respectively. The wetting behavior on both types of surfaces is significantly modified towards more hydrophobic character compared to the flat surface presented in *Figure 12a*, when all surfaces are made of the same material (fluoro-acrylates). Our experiments did not give the definite answer of which surface between those presented in *Figures 12b* and *12c* is more hydrophobic. Both surfaces, nano-structured surfaces only and micro-structured surface only, have shown similar water contact angles. There were cases, when the nano-structures, generated by reactive ion etching of smooth surfaces, showed slightly higher contact angles than certain micro-structures, while in other cases, when different micro-structures (usually with smaller period and size) were assessed, higher water contact angles were measured for them than for the nano-structured surface. However, the combination of dual-scale surface structures (micro- and nano-structures), made in the given fluoro-acrylate material, has shown the highest value for the water contact angle (*Figure 12d*). Without any further experimental evidence, it is believed that such dual structures allowed the most air to be trapped under the water drops, which contributed to both, the superhydrophobic and the self-cleaning behavior. Particularly, the dual structure topographies minimize the contact points between the water drops and the surface [71,85-87].

The randomly-texturized surfaces, which SEM images are presented in *Figure 5*, showed better repellent behavior than the smooth surfaces made from the same material (fluoro-acrylates). Better repellency was observed for smaller surface features (*Figure 5a*) than the larger random counterparts (*Figure 5b*). Compared to the well-defined micro-structured or

dual-structure topographies, in general, the surfaces with random features showed lower contact angles. However, the surfaces with smaller random features were very close in terms of their contact angles and sliding angles to several of well-defined patterned topographies, especially those with smaller feature sizes and periods.

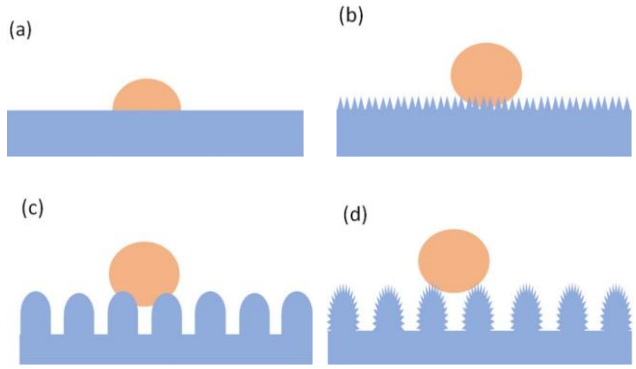

Figure 12. Drop of water on: (a) flat surface; (b) nano-structured surface; (c) micro-structured surface; and (d) micro-/nano-structured surface.

The micro-size structures were systematically changed in terms of their size and periodicity, as shown in *Figure 8*. A trend towards improved non-wetting and self-cleaning behavior was observed, when the feature size and period were compared relative to the water drop size. These results will be published additionally. For the purpose of this report, the authors believe that the extensive results on quantitative assessment of superhydrophobicity and self-cleaning character are beyond the primary goal of the study, which is to present the versatility and capabilities of soft lithography.

The main observations regarding superhydrophobic and self-cleaning topographies, fabricated and tested in this part of the study, can be recapitulated as follows:

- For all topographies developed in this study, the water contact angle was used as a quantitative measure for the superhydrophobic character of tested surfaces, while the sliding angle was used as a measure for self-cleaning performance.
- The ***water contact angle*** was found to increase by incorporation of micron-size features on a surface made of low surface energy material compared to a smooth surface or randomly-texturized surface of the same material. Further increase in the water contact angle was observed for the hierarchical dual-structure topographies. All tested topographies have shown water contact angles above 140°.
- The ***sliding angle*** was found to decrease by introducing micro-structured topography and was further decreased by incorporation of nano-structures on top of the existing surface micro-structures. All tested surfaces have exhibited sliding angles in the range 3^{o}-8^{o}.
- It is believed that the combination of dual-scale surface structures and low surface energy materials minimize the contact points and allows air to be trapped between the drops and the surface, which is responsible for both, the superhydrophobic and the self-cleaning behavior.

IV. CONCLUSION

Soft lithography provides a low-expertise and quick route towards fabrication of micro- and nano-patterned engineered topographies, making it as one of the top listed and most versatile tool without major capital equipment investment.

Surface patterns in this work were successfully developed and fabricated by soft lithographic replica molding technique using an acrylate stamp. The first category of surface patterns developed in this report were anti-fouling topographies, which have shown increased inhibition of bacterial attachment and biofim formation compared to randomly-texturized or smooth surfaces. The second category of topographies developed and tested in this work were hydrophobic topographies, which showed improved non-wetting and self-cleaning behavior compared to random texture and smooth surfaces. The surface patterns' size and pitch, i.e. the specific surface area seem to play the major role in the surface final performance. The quantitative results of the anti-fouling and self-cleaning surface assessment will be published additionally.

It is believed that the qualitative observations made in this work, coupled with the quantitative (kinetic study) results, which will follow soon, will contribute towards:

- better understanding of biofilm formation on structured topographies and will provide further knowledge into design of anti-fouling surfaces, and
- better insight into surface factors responsible for the non-wetting and self-cleaning behavior of structured hydrophobic surfaces.

REFERENCES

[1] Y. Xia, G. M. Whitesides, Angew. Chem. Int. Ed. **37** (1998) 550.
[2] X.-M. Zhao, Y. Xia, G. M. Whitesides, J. Mater. Chem. **7**(7) (1997) 1069.
[3] D. Qin, Y. Xia & George M Whitesides, Nature Protocols **5**(3) (2010) 491.
[4] D.J. Lipomi, R.V. Martinez, L. Cademartiri, G.M. Whitesides, Polymer Science: A Comprehensive Reference **7** (2012**)** 211.
[5] D. B. Weibel, W. R. DiLuzio, G. M. Whitesides, Nature Reviews – Microbiology **5** (2007) 209.
[6] G. M. Whitesides, E. Ostuni, S. Takayama, X. Jiang, [7] D. E. Ingber, Annu Rev Biomed. Eng. **3** (2001) 335.
[7] L. R. Freschauf, J. McLane, H. Sharma, M. Khine, PLOS ONE **7**(8) (2012) e40987.
[8] H. M. Saavedra1, T. J. Mullen, P. Zhang, D. C. Dewey1, S. A. Claridge, P. S. Weiss, Rep. Prog. Phys. **73** (2010) 036501.
[9] J. A. Rogers , R. G. Nuzzo, MaterialsToday **8**(2) (2005) 50.
[10] J. P. Urbanski, W. Thies, C. Rhodes, S. Amarasingheb,T. Thorsen, Lab Chip **6** (2006) 96.
[11] C. R. Martin, I. A. Aksaya, J. Mater. Res. **20**(8) (2005) 1995.
[12] A. L. Thangawng, M. A. Swartz, M. R. Glucksberg, R. S. Ruoff, Small **3**(1) (2007) 132.
[13] P. Kim, K. Woo Kwon, M. C. Park, S. H. Lee, S. M. Kim, K. Y. Suh, Biochip Journal **2**(1) (2008) 1.
[14] T. M. Nargang, L. Brockmann, P. M. Nikolov, D. Schild, D. Helmer, N. Keller, K. Sachsenheimer, E. Wilhelm, L. Pires, M. Dirschka, A. Kolew, M. Schneider, M. Worgull, S. Giselbrecht, C. Neumann, B. E. Rapp, Lab Chip **14** (2014) 2698.
[15] D. J. Eichelsdoerfer, X. Liao, M. D. Cabezas, W. Morris, B. Radha, K. A. Brown, L. R. Giam, A. B. Braunschweig, C.A. Mirkin, Nature Protocols **8** (2013) 2548.
[16] C. R. Martin, I. A. Aksaya, J. Mater. Res. **20** (8) (2005).
[17] M. Brehmer, L. Conrad, L. Funk, J. Disp. Sci. and Technol. **24**(3 & 4) (2003) 291.
[18] M. H. Lee, M. D. Huntington, W. Zhou‡, J.-C. Yang, T. W. Odom, Nano Lett. **11**(2) (2011) 311.

[19] Y. Huang, G. T. Paloczi, J. Scheuer, A. Yariv, Optics Express **11**(20) (2003) 2452.
[20] J. L. Wilbur, A. Kumar, E. G. Kim, M. Whitesides, Adv. Mater. **6** (1994) 600.
[21] A. Trajkovska Petkoska, Polymer Cholesteric Liquid Crystal Flakes–Their Electro Optic-Behaviour for Potential E-Paper Application, VDM ISBN 978-3-639-06439-1, Germany 2008.
[22] G.M. Kappell, J. P. Grover, T. H. Chrzanowski, Elec. J. Biotechnology **12**(3) (2009) 1.
[23] E. Kujundzic, A. C. Fonseca, E. A. Evans, M. Peterson, A. R. Greenberg, M. Hernandez, J. Microbiol. Methods **68** (2007) 458.
[24] A. K. Wessel, L. Hmelo, M. R. Parsek, M. Whiteley, Nature Reviews – Microbiology **11** (2013), 337.
[25] R. M. Donlan, Emerging Infectious Diseases **8**(9) (2002) 881.
[26] B. Prakash, B. M. Veeregowda, G. Krishnappa, Current Science **85**(9) (2003) 1299.
[27] S. Stepanovic, I. Cirkovic, L. Ranin, M. S. Vlahovic, Lett. in Appl. Microbiol. **38** (2004) 428.
[28] R. M. Harshey, Annu. Rev. Microbiol. **57** (2003) 249.
[29] K. Sauer, A. H. Rickard, D. G. Davies, Microbe **2**(7) (2007) Y347.
[30] N. Verstraeten, K. Braeken, B. Debkumari, M. Fauvart, J. Fransaer, J. Vermant, J. Michiels, Trends in Microbiology **16**(10) (2008) 497.
[31] R. Van Houdt, C. W. Michiels, Research in Microbiology **156** (2005) 626.
[32] L. Daneshmehr, K. Matin, T. Nikaido, J. Tagami, J. Dentistry **36** (2008) 33.
[33] Z. M. Thein, Y. H. Samaranayake, L.P. Samaranayake, Arch. of Oral Biology **52** (2007) 1200.
[34] M. Ono, T. Nikaido, M. Ikeda, S. Imai, N. Hanada, J. Tagami, K. Matin, Dental Mat. J. **26**(5) (2007) 613.
[35] C. M. Manuel, O. C. Nunes, L. F. Melo, Water Research **41** (2007) 551.
[36] F. Teng, Y.T. Guan, W.P. Zhu, Corrosion Science **50** (2008), 2816.
[37] M. Hocevar, M. Jenko, M. Godec, D. Drobne, Mater. and Technol. **48**(5) (2014) 609.
[38] A. Hammond, J. Dertien, J. A. Colmer-Hamood, J. A. Griswold, A. N. Hamood, J. Surgical Research 1–12 (2009).
[39] L.A. Mermel, Emerging Infectious Diseases **7**(2) (2001) 197.
[40] J. O. Falkinham, J. Medical Microbiology **56** (2007) 250.
[41] R. M. Dominic, S. Shenoy, S. Baliga, Kathmandu University Medical Journal **5**(3) (2007) 431.
[42] M. Simoces, L. C. Simoces, M. J. Vieira, Food Sci. Techn. **43** (2010) 573.
[43] M. V. Graham, N. C. Cady, Coatings **4** (2014) 37.
[44] H. Otsuka, Molecules **15** (2010) 5525.
[45] I. Francolini, P. Norris, A. Piozzi, G. Donelli, P. Stoodley, Antimicrobial Agents and Chemotheraphy (2004) 4360.
[46] W. C. Chiang, C. Schroll, L. R. Hilbert, P. Møller, T. T.-Nielsen, Appl. Environ. Microbiology (2009) 1674.
[47] D. Y. Lyon, D. Browna, E. R. Sundstromb, P. J.J. Alvarez. Intern. Biodeterioration & Biodegradation **62** (2008) 475.
[48] G. Guerrero, J. Amalric, P.-H. Mutin, A. Sotto, J.-P. Lavigne, Pathologie Biologie **57** (2009) 36.
[49] H. Zhang, J. Tang, X. Meng, J. Tsang, T.-K. Tsang, Digestive Diseases and Sciences **50**(6) (2005) 1046.
[50] R. M. May, M. G. Hoffman, M. J. Sogo, A. E. Parker, G. A. O'Toole, A. B. Brennan, S. T Reddy, Clinical and Translational Medicine **3**(8) (2014).
[51] P. N. Danese1, Chemistry & Biology **9** (2002) 873.
[52] K. Koch, W. Barthlott, Phil. Trans. R. Soc. A (2009) 367.
[53] S. H. Nguyen, H. K. Webb, P. J. Mahon, R. J. Crawford, E. P. Ivanova, Molecules **19** (2014) 13614.
[54] B. Bhushan, Beilstein J. Nanotechnol. **2** (2011) 66.
[55] M. Nosonovsky, B. Bhushan, Microelectronic Eng. **84** (2007) 382.
[56] B. Bhushan, Phil. Trans. R. Soc. A **367** (2009) 1445.
[57] W. Barthlot, T. Schimmel, S. Wiersch, K. Koch, M. Brede, M. Barczewski, S. Walheim, A. Weis, A. Kaltenmaier, A. Leder, H. F. Bohn, Adv. Mater. **22** (2010) 2325.
[58] B. Bhushan, Y. C. Jung, K. Koch, Phil. Trans. R. Soc. A **367** (2009) 1631.
[59] A. J. Schulte, D. M. Droste1, K. Koch, W. Barthlott, Beilstein J. Nanotechnol. **2** (2011) 228.
[60] Y. C. Yung, Natural and Biomimetic Artificial Surfaces for Superhydrophobicity, Self-Cleaning, Low Adhesion, and Drag Reduction, PhD Thesis, The Ohio State University, 2009.
[61] M. Nosonovsky, B. Bhushan, Curr. Opinion in Coll. & Interface Sci., **14** (2009) 270.
[62] M. Ma, R. M. Hill, Curr. Opinion in Coll. & Interface Sci. **11** (2006) 193.
[63] L. Raibeck, J. Reap, B. Bras, CIRP J. Manuf. Sci.and Technol. **1** (2009) 230.
[64] R. Hensel1, R. Helbig, S. Aland, A. Voigt, C. Neinhuis, C. Werner, NPG Asia Materials **5** (2013) e37.
[65] F. E. Fish, Bioinsp. Biomim. **1** (2006) R17.
[66] W. Sagong, C. Kim, S. Choi, W.-P. Jeon, H. Choia, Phys. of Fluids **20** (2008) 101510.
[67] M. Vlachogiannis, T. J. Hanratty, Exper. in Fluids **36** (2004) 685.
[68] R. J. Daniello, N. E. Waterhouse, J. P. Rothstein, Phys. of Fluids **21** (2009) 085103.
[69] S. M. Lee, T. H. Kwon, Nanotechnology **17** (2006) 3189.
[70] C. Neinhuis, W. Barthlott, Annals of Botany **79** (1997) 667.
[71] K. Koch, B. Bhushan, Y. C. Jung, W. Barthlott, Soft Matter. **5** (2009) 1386.
[72] J. Zhang, J. Wang, Y. Zhao, L. Xu, X. Gao, Y. Zheng, L. Jiang, Soft Matter. **4** (2008) 2232.
[73] S. S. Latthe, C. Terashima, K. Nakata, A. Fujishima, Molecules **19** (2014) 4256.
[74] J. Wang, H. Chen, T. Sui, A. Li, D. Chen, Plant Science **176** (2009) 687.
[75] V. Zorba, E. Stratakis, M. S. Barberoglou, E. Spanakis, P. Tzanetakis, S. H. Anastasiadis, C. Fotakis, Adv. Mater. **20** (2008) 4049.
[76] Y. T. Cheng, D. E. Rodak, Appl. Phys. Lett. **86** (2005) 144101.
[77] X. M. Li, D. Reinhoudt, M. C. Calama, Chem. Soc. Rev. **36** (2007) 1350.
[78] S. H. Hsu, W. M. Sigmund, Langmuir **26**(3) (2010) 1504.
[79] X. Lu, Y. Jin, S. Tan, L. Zhang, Y. Liu, X. Zhang, J. Xu, J. Adh. Sci. Technol. **22** (2008) 1841.
[80] I. P. Parkin, R. G. Palgrave, J. Mater. Chem. **15** (2005) 1689.
[81] J. Fresnais, J. P. Chapel, L. Benyahia, F. P. Epaillard, J. Adh. Sci. Technol. **23** (2009) 447.
[82] S. Gogte, P. Vorobieff, R. Truesdell, A. Mammoli, F. van Swoll, P. Shah, Phys. Fluids, **17** (2005) 051701.
[83] J. Heikenfeld, M. Dhindsa, J. Adh. Sci. Technol. **22** (2008) 319.
[84] Y. Zheng, L. Jiang, J. Wang, D. Han, Appl. Phys. Lett. **93** (2008) 094107.
[85] S. Moulinet, D. Bartolo, Eur. Phys. J. E **24** (2007) 251.
[86] K. Koch, B. Bhushan, W. Barthlott, Soft Matter **4** (2008) 1943.
[87] D. Quere, Annu. Rev. Mater. Res. **38** (2008) 71.
[88] B. Balu, J. S. Kim, V. Breedveld, D.W. Hess, J. Adh. Sci. Technol. **23** (2009) 361.
[89] J. Wang, Y. Yu, D. Chen, Chinese Science Bulletin **51** (19) (2006) 2297.
[90] S J Abbott, P H Gaskell, Proc. IMechE **221** Part C: J. Mechan. Eng. Sci., Spec. Iss. (2007) 1181.
[91] R. Truesdell, A. Mammoli, P. Vorobieff, F. Swol, C. J. Brinker, Phys. Rev. Lett. PRL **97** (2006) 044504.
[92] S. H. Kim, J. Adh. Sci. Technol. **22** (2008) 235.
[93] H. M. Shang, Y. Wang, K. Takahashi, G. Z. Cao, J. Mater. Sci. **40** (2005) 3587.
[94] Y. C. Jung, B. Bhushan, J. Microscopy **229**(1) (2008) 127.
[95] X. Han, D. Y. Zhang, X. Li, Y. Y. Li, Chinese Science Bulletin **53**(10) (2008) 1587.
[96] P. Roach, N. J. Shirtcliffe, M. I. Newton, Soft Matter. **4** (2008) 224.
[97] J. Xi, L. Feng, L. Jiang, Appl. Phys. Lett. **92** (2008) 053102.
[98] Y. Zhou, X. Song, M. Yu, B. Wang, H. Yan, Surf. Rev. Lett. **13**(1) (2006) 117.